The Astrophysical Journal, 705:1632–1636, 2009 November 10 doi:10.1088/0004-637X/705/2/1632

THE LUMINOSITY FUNCTION OF X-RAY SOURCES IN SPIRAL GALAXIES

A. H. Prestwich[1], R. E. Kilgard[2], F. Primini[1], J. C. McDowell[1], and A. Zezas[1,3]
[1] Harvard-Smithsonian Center for Astrophysics, Cambridge, MA 02138, USA
[2] Wesleyan University, Middletown, CT 06459, USA
[3] Physics Department, University of Crete, Heraklion, Greece
Received 2008 November 14; accepted 2009 September 29; published 2009 October 26

ABSTRACT

X-ray sources in spiral galaxies can be approximately classified into bulge and disk populations. The bulge (or hard) sources have X-ray colors which are consistent with low-mass X-ray binaries (LMXBs) but the disk sources have softer colors suggesting a different type of source. In this paper, we further study the properties of hard and soft sources by constructing color-segregated X-ray luminosity functions (XLFs) for these two populations. Since the number of sources in any given galaxy is small, we co-added sources from a sample of nearby, face-on spiral galaxies observed by *Chandra* as a Large Project in Cycle 2. We use simulations to carefully correct the XLF for completeness. The composite hard source XLF is not consistent with a single-power-law fit. At luminosities $L_x > 3\times10^{38}$ erg s^{-1}, it is well fitted by a power law with a slope that is consistent with that found for sources in elliptical galaxies by Kim & Fabbiano. This supports the suggestion that the hard sources are dominated by LMXBs. In contrast, the high-luminosity XLF of soft sources has a slope similar to the "universal" high-mass X-ray binary XLF. Some of these sources are stellar-mass black hole binaries accreting at high rates in a thermal/steep power-law state. The softest sources have inferred disk temperatures that are considerably lower than found in galactic black holes binaries. These sources are not well understood, but some may be super-soft ultra-luminous X-ray sources in a quiescent state as suggested by Soria & Ghosh.

Key words: galaxies: spiral – galaxies: starburst – surveys – X-rays: galaxies – X-rays: general

Online-only material: color figures

1. INTRODUCTION

It has been known for three decades that nearby spiral galaxies contain a multitude of X-ray sources (van Speybroeck et al. 1979). Observations of the Milky Way and Local Group galaxies have shown that the brightest of these sources are low-mass X-ray binaries (LMXBs). In these systems, material is transferred at a high rate via Roche lobe overflow from a low-mass star onto a compact companion (a white dwarf, neutron star, or black hole). Their X-ray spectra are broadly characterized by a power law with photon index $\gamma \sim 2.5$ (Tanaka 1997). High-mass X-ray binaries (HMXBs) are powered by Bondi–Hoyle accretion from the stellar winds of a young, high-mass star onto a compact object. They typically have much harder spectra than LMXBs (photon index $\gamma = 0$–1.5; Haberl & Pietsch 2004). The accretion rates are lower than for Roche lobe overflow sources and the corresponding X-ray luminosities are also lower (White 1989). In addition to the basic classification depending on the mass of the secondary, many other groups of sources have been identified depending on their X-ray spectra and variability properties. For example, the so-called super-soft sources (SSSs), believed to be binaries with white dwarf primaries accreting matter at a highly super-Eddington rate (Greiner et al. 1991), have essentially all of their flux below 1 keV, and are highly variable (Di Stefano & Kong 2003; Di Stefano et al. 2004). Supernova remnants are also known to be strong X-ray sources (Reynolds 2008). For a review of X-ray sources in galaxies see Fabbiano (2006).

In the closest galaxies, clues as to the nature of X-ray sources can be derived from the optical environments and/or counterparts (Kilgard et al. 2006; Trudolyubov et al. 2005). However, it is more difficult to identify X-ray sources in galaxies which are too distant for optical counterparts to be detected and where there are not enough counts to get an X-ray spectrum. In Prestwich et al. (2003), we suggested that X-ray colors are a good starting point for source classification. We found that the X-ray colors of the sources described above (low- and high-mass binaries, SSSs, and supernova remnants (SNRs)) lie in different parts of the X-ray color–color diagram, albeit with some overlap of source types. In particular, sources in elliptical galaxies and spiral bulges fall in a well-defined region of the X-ray color–color diagram. We suggest that this population is dominated by LMXBs. We find very few sources with hard HMXB colors, which is to be expected given their low X-ray luminosities. We also find a population of faint X-ray soft sources in disk galaxies not seen in bulges. These soft/thermal sources are clearly associated with star formation, and are likely a mix of supernova remnants and accretion-powered sources (see also Di Stefano et al. 2004).

In this paper, we further investigate the properties of hard (or LMXBs) and soft sources by constructing color-segregated X-ray luminosity functions (XLFs). Our motivation is to confirm our interpretation that the hard sources are dominated by LMXBs and to better understand the mix of objects that fall into the soft class. In Section 2, we describe our galaxy sample and completeness simulations, and in Section 3 we describe fits to hard and soft sources. In Section 4, we compare our results to previous work and discuss the origin of soft sources. Our conclusions are summarized in Section 6.

2. GALAXY SAMPLE AND SIMULATIONS

Most spiral galaxies have 10–50 X-ray sources, so that it is impossible to construct statistically significant color-segregated luminosity functions for a single galaxy. We therefore constructed color-segregated XLFs by co-adding hard and soft sources from 11 spiral galaxies. The galaxies chosen for this work were observed as a *Chandra* Large Project in Cycle 2 (see Kilgard et al.

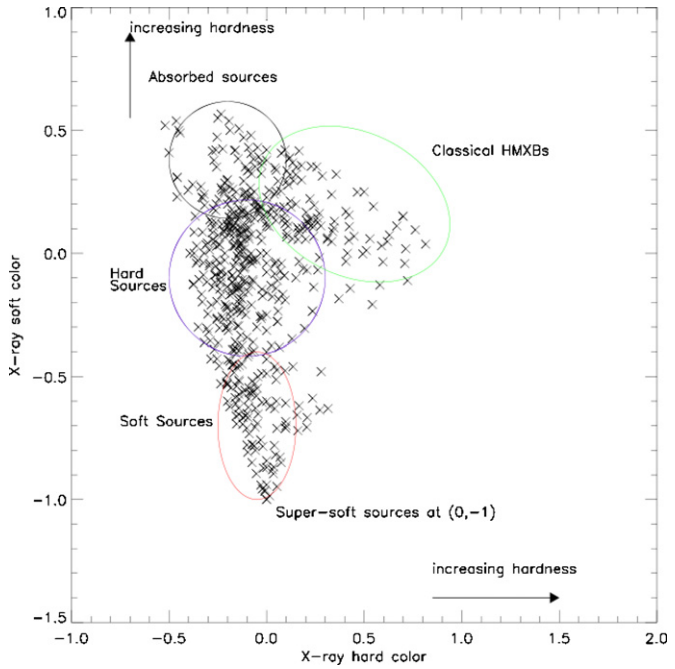

Figure 1. X-ray color–color diagram for sources in spiral galaxies from Prestwich et al. (2003). The location of hard and soft sources is shown.

(A color version of this figure is available in the online journal.)

2005 for details of data reduction and a complete source list). They are all nearby (< 10 Mpc), face on spirals with low foreground absorption. The X-ray colors of sources in this sample are therefore relatively insensitive to patchy local absorption and the inclination of the galaxy. We use color definitions hard color (HC) and soft color (SC) introduced by Prestwich et al. (2003):

$$\mathrm{HC} = \frac{H - M}{T}$$

$$\mathrm{SC} = \frac{M - S}{T}.$$

Here, H, M, and S are counts in the soft (0.3–1 keV), medium (1–2 keV), and hard (2–8 keV) bands, respectively, and $T = S + M + H$. We define soft and hard source colors as follows:

$$\text{soft color} : \mathrm{SC} < 0.4$$

$$\text{hard color} : -0.4 < \mathrm{SC} < 0.2, -0.3 < \mathrm{HC} < 0.4.$$

These regions are shown on a color–color diagram in Figure 1.

The composite XLFs for soft and hard sources are shown in Figures 2 and 3. An inspection of these figures suggests that the soft sources are well represented by a single power law. In contrast, the XLF of the hard sources starts to flatten at $L_x \sim 3\times10^{38}$ erg s^{-1}. The flattening of the XLF may be due to a real change in the properties of the sources or an artifact due to incompleteness (or a combination of both). There are several factors that affect the detection threshold for X-ray sources, including the presence of diffuse emission and the distance of the source from the aim point. In addition, ACIS-S was significantly more sensitive to soft emission (<1 keV) in Cycle 2 than to harder sources; this will result in a different completeness limit for hard and soft sources. We construct simulated XLF to help distinguish between a real break in the XLF and incompleteness effects.

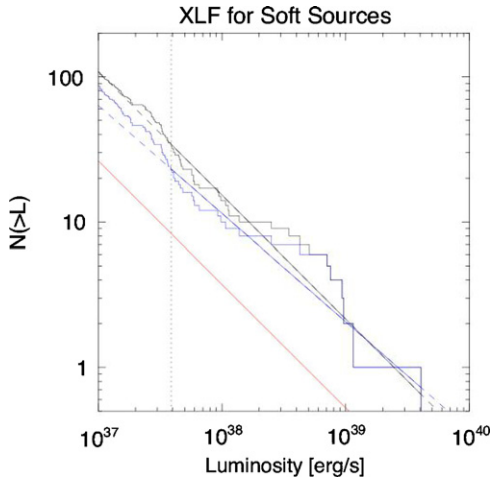

Figure 2. XLFs for soft sources. The black curves show the data and best-fit power law, the red line shows the distribution of background sources and the blue curves the background-corrected XLFs. The vertical dotted line shows the completeness limit. Points below the completeness limit were not included in the fit.

(A color version of this figure is available in the online journal.)

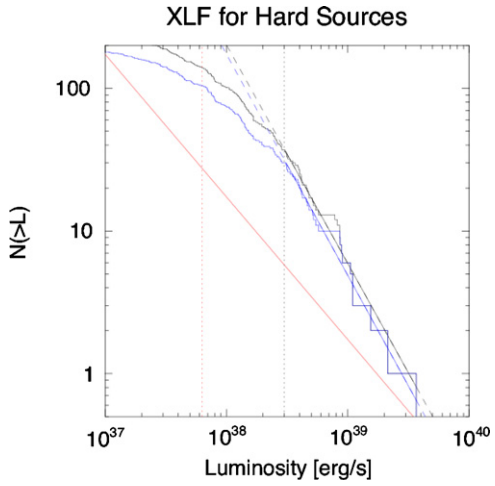

Figure 3. XLF for hard sources. The black curves show the data and best-fit power law, the red line shows the distribution of background sources and the blue curves the background-corrected XLFs. The red vertical dotted line shows the completeness limit. The black vertical line shows the lowest luminosity included in the fit.

(A color version of this figure is available in the online journal.)

We use the "backward" method described by Kim & Fabbiano (2004) to ascertain the completeness limit of each galaxy for a given source type (hard or soft). This method involves simulating a source with the appropriate spectrum, and adding the simulated source to the real galaxy data. The source detection algorithm used for the original galaxy source list is then run again to determine whether the "fake" source is detected. Approximately 20,000 soft sources and 20,000 hard sources are added to each galaxy, sprinkled randomly over the area within D_{25}. We use a power law of photon index 1.2 to simulate hard sources and a power law of photon index 3.0 to simulate soft sources. The detected algorithm was run on the full band image, as was also the case for the galaxy analysis. The ratio of the number of the input to the number of the detected sources at a given luminosity is the key factor: when this falls below 100% the sample is not complete. In order to construct a composite XLF, we added sources to luminosity bins where

Table 1
Completeness Limits for Hard Sources

Luminosity ($\times 10^{38}$ erg s^{-1})	NGC 4314	NGC 1291	NGC 3184	M94
0.75	20% (5)	50% (4)	50% (1)	70% (1)
0.95	50% (2)	68% (1)	70% (1)	90% (1)
1.15	60% (1)	77% (1)	80% (0)	100% (0)
1.35	80% (0)	90% (0)	90% (1)	100% (0)
1.5	90% (1)	100% (0)	100% (0)	100% (0)

Notes. Table gives completeness as a percentage of the input sources detected. The number in parentheses is the number of sources added to the XLF to account for completeness. Galaxies not listed are complete down to 7.5×10^{37} erg s^{-1}.

the completeness fell below 100%. For each galaxy, sources were added to the XLF according to the following formula:

$$N_{\rm add}(L) = \frac{(1-F)}{F} N_{\rm gal}(L). \quad (1)$$

Here, $N_{\rm add}(L)$ is the number of sources added to the bin of luminosity L and F is the fractional completeness, defined as the ratio of the number of the input to the number of the sources detected in simulations. $N_{\rm gal}(L)$ is the number of the real sources in the galaxy with luminosity L.

We find that the soft source population is 100% complete down to 3.9×10^{37} erg s^{-1} for most galaxies (M101, IC 5332, M94, M51, M83, NGC 2681, M74, and NGC 1291). No sources were added to the XLF for these galaxies. We omit galaxies NGC 4314, NGC 3184, and NGC 278 from the soft source composite XLF because they are less than 40% complete at 3.9×10^{37} erg s^{-1}. Detection of hard sources was complete down to 7.5×10^{37} erg s^{-1} for galaxies IC 5332, M101, M51, M83, NGC 2681, NGC 278, and NGC 628. Sources were added to the lowest luminosity bins of the remaining galaxies as summarized in Table 1. In addition to correcting for completeness in the lowest luminosity bins, we also removed bright nuclear sources from the composite XLFs. In many cases, these are weak LINERS and not X-ray binaries.

3. FITS TO COMPOSITE XLFs

The method used for fitting is described by Kilgard et al. (2005) and full details can be found in that paper. Here, we give a brief summary of the procedure.

We fit a single power law to the unbinned, differential, composite XLFs using a maximum likelihood statistic (Crawford et al. 1970). The XLFs were corrected for completeness as described in the previous section. The single power law has the functional form

$$\frac{dN}{dL_X} \sim L_X^{-\gamma}. \quad (2)$$

The goodness-of-fit (GOF) estimate is performed by simulating a luminosity distribution with the best-fit slope. One million iterations were performed. If the data are well fitted by a single power law, the GOF statistic approaches 1.0. The contribution of cosmic background sources to the XLF was evaluated using the log N–log S curves of Giacconi et al. (2001). The soft band was used for the soft sources and the hard band for the hard sources. We fit down to the completeness limit (3.9×10^{37} erg s^{-1}) for soft sources. It is impossible to fit a single power law from the completeness limit to the highest luminosity source for the hard sources. We therefore fit a single power law above 3×10^{38} erg s^{-1}. Figures 2 and 3 show the composite XLF and best-fit power law (black curves) for soft and hard sources. Also shown is the slope representing the background source distribution (red curve) and the background subtracted data and best fit (blue curve). Best-fit parameters to the composite XLF are shown in Table 2.

4. THE X-RAY SOURCE POPULATION IN SPIRAL GALAXIES

There are two basic conclusions to be drawn from the results presented in the previous section. The first is that although the completeness limit for a given observation depends on many factors, such as diffuse emission, it is lower for soft sources than for hard sources. The second is that there appears to be a break in the hard source XLF at about $\sim3\times10^{38}$ erg s^{-1}. The flattening of the hard source XLF shown in Figure 3 at low luminosities ($<7\times10^{37}$ erg s^{-1}) is largely due to incompleteness.

4.1. Hard Sources

In Prestwich et al. (2003), we suggest that the hard sources are dominated by LMXBs. The XLF of sources in elliptical galaxies, which are almost exclusively LMXBs, has been studied in depth by Kim & Fabbiano (2004) and Gilfanov (2004). Kim & Fabbiano (2004) find that the XLF of a sample of 14 elliptical galaxies (corrected for incompleteness) can be fitted with a single power law, $\gamma = 1.9$ over the range $2\times10^{37} - 2\times10^{39}$ ergs s^{-1}. Although not formally required, a broken power law gives a better fit ($\gamma_1 = 1.8 \pm 0.2$, $\gamma_2 = 2.8 \pm 0.6$) with a break luminosity of $L_b = 5\times10^{38}$ erg s^{-1}. Our fits to the hard sources show very similar features: an XLF which steepens at a few $\times10^{38}$ erg s^{-1}. Our fit parameters are consistent with those of Kim & Fabbiano (2004), albeit with large uncertainties due to a smaller sample. It is likely that we are sampling the same population as Kim & Fabbiano (2004).

4.2. Soft Sources

In Prestwich et al. (2003), we suggested that many of the soft sources are thermal SNRs. We stress here that most of the soft sources considered in Prestwich et al. (2003) have luminosities $<1.0\times10^{37}$ erg s^{-1}. They are below the completeness limit for the composite XLF derived here. The soft sources at the high-luminosity end of the XLF are almost certainly dominated by accretion-powered sources. The association of soft sources with star formation strongly suggests that the donor stars are young supergiant, O, or B stars, even though the SCs of these binaries is very different from the hard spectra of wind-accretion sources described in Section 1. We therefore compare the XLF of soft sources to that of HMXB. The nature of the soft sources is discussed further in Section 5.

The XLF of high-mass binaries in star-forming galaxies has been studied in detail by Grimm et al. (2003). They find that the HMXB XLF is well described by a single power law ($\gamma = 1.61 \pm 0.12$) over the luminosity range 10^{35}–10^{40} ergs s^{-1}. The slope derived by Grimm et al. (2003) is very close to our best-fit single power law for soft sources ($\gamma = 1.73 \pm 0.15$), suggesting that we are sampling the same population.

5. THE NATURE OF THE SOFT SOURCES

As discussed above, the luminous soft sources discussed here are most likely HMXBs. However, they are clearly more luminous and have much softer spectra than wind-fed HMXBs (binary pulsars) found in the Milky Way and Local Group

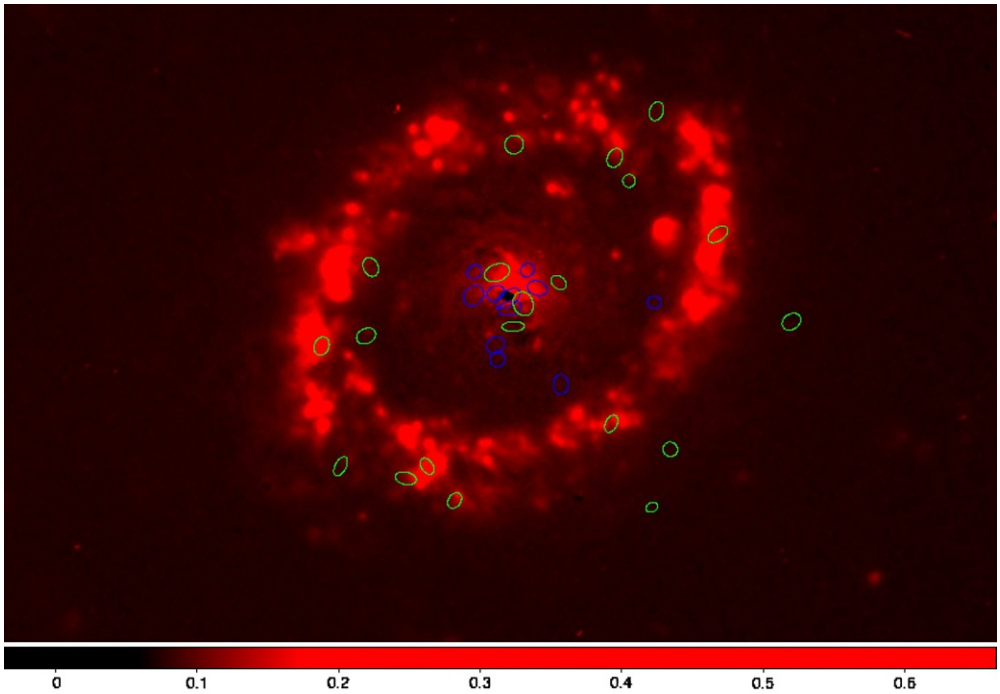

Figure 4. Hα image of the center of NGC 4736 showing the star-forming ring. Positions of soft X-ray sources are plotted in green and hard sources are plotted in blue. The soft sources are predominantly associated with the ring.
(A color version of this figure is available in the online journal.)

Table 2
Power-law Fits to Composite, Corrected XLFs

Sample	γ	$\gamma_{\rm corr}$	$L_{\rm low}$ (10^{37} erg s^{-1})	$L_{\rm comp}$ (10^{37} erg s^{-1})	GOF	$N_{\rm fit}$	$N_{\rm comp}$	$N_{\rm tot}$
Soft	1.82 ± 0.14	1.73 ± 0.15	3.9	3.9	0.7	32	32	170
Hard	2.53 ± 0.25	2.55 ± 0.28	30.0	7.5	1.05	37	104	236

Notes. Power-law fits to composite, corrected XLFs. γ is the fitted slope to the XLF with no background correction, $\gamma_{\rm corr}$ correcting for background sources. $L_{\rm low}$ is the low luminosity used in the fit, $L_{\rm comp}$ is the completeness limit. GOF is the goodness-of-fit parameter and $N_{\rm fit}$ is the number of sources included in the fit. $N_{\rm comp}$ is the number of sources above the completeness limit and $N_{\rm tot}$ is the total number of detected sources.

galaxies. The higher luminosities suggest that the soft sources are accreting material at a higher rate than is found in wind-fed HMXBs. This requirement, plus the softer spectra, suggests that the accretion mechanism is fundamentally different than galactic HMXB. In this section, we discuss the nature of these sources in more detail.

The association of the soft sources with star formation is clearly demonstrated in the case of NGC 4736 (M94). This galaxy has a circumnuclear ring of star formation (Waller et al. 2001). Figure 4 shows the Hα image of this galaxy with the positions of soft (green) and hard (blue) X-ray sources. It is clear that the soft sources are found primarily in the star-forming ring. Given the association with star formation, these sources are most plausibly neutron star or black hole X-ray binaries with young stellar companions. The X-ray spectral states of black hole X-ray binaries have been described in detail by Remillard & McClintock (2006). In the low accretion state, the X-ray emission is dominated by a hot corona. As the accretion rate increases, the X-ray flux comes primarily from a disk and is thermal in origin. The emission is characterized by a disk-blackbody spectrum ($kT \sim 1$ keV) with some contribution at higher energies from a power-law component. In the highest accretion state (steep power law, or SPL), the X-ray emission is characterized by a soft power law ($\Gamma > 2.5$). Figure 5 shows the X-ray color–color diagram from Prestwich et al. (2003) for all detected sources, with thermal and SPL models plotted for reference. The red curve shows the colors of disk-blackbody models for inner disk temperatures of 0.1–1.1 keV. Adding a power-law component to a disk-blackbody has the effect of moving the colors up and to the left of the diagram, as demonstrated by the green points. The purple points show a simple power law, representing the SPL state.

Figure 5 shows that some of the soft sources have colors that are very similar to black holes accreting in the thermal or SPL state. However, some of the softest sources have disk temperatures that are much cooler ($kT \sim 0.1$–0.3 keV) than is typically found in galactic black hole binaries ($kT \sim 1$ keV). Low disk temperatures have also been observed in ultra-luminous X-ray sources (ULXs). Since $M \sim T_{\rm in}^{-2}$, such low disk temperatures have been used to suggest that ULXs contain intermediate-mass black holes (IMBHs; e.g., Makishima et al. 2000). It seems very unlikely that we are observing a population of IMBHs. If the mass of the black holes is $\sim 100\,M_{\odot}$, the low luminosities (10^{37}–10^{38} erg s^{-1}) would imply sub-Eddington accretion rates. In this case, we would not expect to see thermal emission, which is generally observed when the accretion is

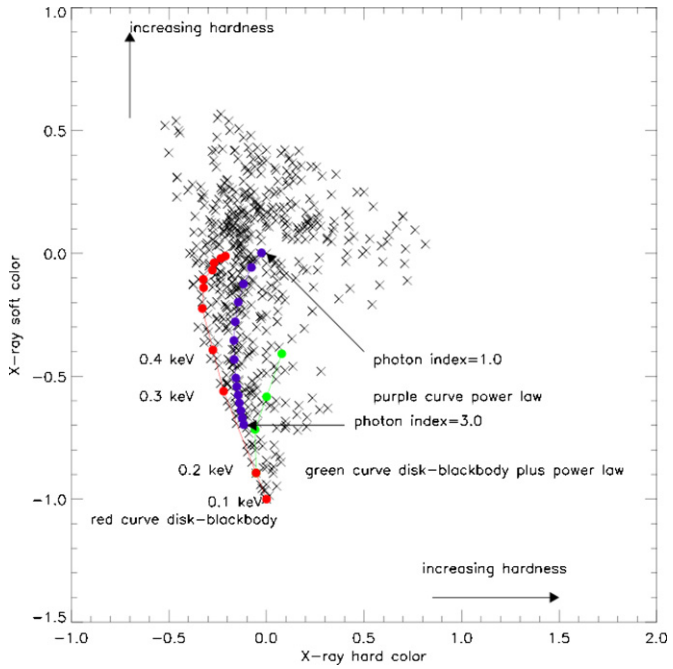

Figure 5. X-ray color–color diagram for sources in spiral galaxies. Curves for thermal and SPL models for black binaries are plotted for reference. The red curve shows the colors of disk-blackbody models for inner disk temperatures of 0.1–1.1 keV. Adding a power-law component to a disk-blackbody has the effect of moving the colors up and to the left of the diagram, as demonstrated by the green points. The purple points show a simple power-law characteristic of sources in the SPL state.

(A color version of this figure is available in the online journal.)

dominated by a disk and the rates are close to Eddington. The combination of soft spectrum and low luminosity displayed by a subset of our soft sources is hard to explain if the sources are IMBHs. If they are stellar-mass black holes, their disk temperatures are unusually low.

Soria & Ghosh (2009) recently discussed a state transition in a ULX in NGC 4631. In the high state, NGC 4631 is a super-soft source. In the low state, observed by *Chandra*, it has a luminosity of $L_x \sim 10^{37}$–10^{38} erg s^{-1} and colors consistent with a thermal temperature of 0.1–0.3 keV. They interpret the ULX/super-soft phase of NGC 4631 as a super-Eddington outburst powered by nuclear burning on the surface of a white dwarf. In its low state, the NGC 4631 ULX is very similar to the soft sources described here. By extension, some of the soft sources in spiral galaxies may be quiescent super-soft ULXs. A detailed study of the variability properties of these sources is required to better understand their nature.

6. SUMMARY AND CONCLUSIONS

In this paper, we construct color-segregated XLFs of hard and soft sources by combining data from a sample of face-on spiral galaxies. Since the number of sources in any given galaxy is small, we co-added sources from a sample of nearby, face-on spiral galaxies. To determine the completeness level of each galaxy as a function of source type (hard or soft), we add "fake" sources to real galaxy data and determine the ratio of fake sources added to the number recovered by source detection routines. If all the fake sources were detected, the galaxy is 100% at that flux level. We added sources to the lowest luminosity bins to produce composite color-segregated XLFs that are complete down to 3.9×10^{37} erg s^{-1} for soft sources and 7.5×10^{37} erg s^{-1} for hard sources.

The composite hard source XLF is best fitted by a broken power law and has a high luminosity slope consistent with that found for sources in elliptical galaxies by Kim & Fabbiano (2004). We conclude that the hard population is dominated by LMXB. The soft XLF above the completeness limit is very similar to the "universal" HMXB XLF described by Grimm et al. (2003). This strongly suggests that although thermal SNRs contribute to the soft population at lower luminosities, the high-luminosity end of the XLF is dominated by accretion-powered HMXB. The association of soft sources with star formation is confirmed by looking in detail at NGC 4736, where the soft sources are coincident with a ring of Hα emission. Some of these sources are stellar-mass black hole binaries accreting in the thermal/PL states. However, the softest sources have inferred disk temperatures that are considerably lower than those found in galactic black holes binaries. These sources are not well understood, but some may be super-soft ULXs in a quiescent state as suggested by Soria & Ghosh (2009).

This work was supported by NASA contract NAS 8-39073 (CXC) and GO1-2029A. Thanks to an anonymous referee for several very useful suggestions.

REFERENCES

Crawford, D. F., Jauncey, D. L., & Murdoch, H. S. 1970, ApJ, 162, 405
Di Stefano, R., & Kong, A. K. H. 2003, ApJ, 592, 884
Di Stefano, R., et al. 2004, ApJ, 610, 247
Fabbiano, G. 2006, ARA&A, 44, 323
Giacconi, R., et al. 2001, ApJ, 551, 624
Gilfanov, M. 2004, MNRAS, 349, 146
Greiner, J., Hasinger, G., & Kahabka, P. 1991, A&A, 246, L17
Grimm, H.-J., Gilfanov, M., & Sunyaev, R. 2003, MNRAS, 339, 793
Haberl, F., & Pietsch, W. 2004, A&A, 414, 667
Kilgard, R. E., Prestwich, A. H., Ward, M. J., & Roberts, T. P. 2006, in Proc. IAU Symp. 230, Populations of High Energy Sources in Galaxies, ed. E. J. A. Meurs & G. Fabbiano (Cambridge: Cambridge Univ. Press), 189
Kilgard, R. E., et al. 2005, ApJS, 159, 214
Kim, D.-W., & Fabbiano, G. 2004, ApJ, 611, 846
Makishima, K., et al. 2000, ApJ, 535, 632
Prestwich, A. H., Irwin, J. A., Kilgard, R. E., Krauss, M. I., Zezas, A., Primini, F., Kaaret, P., & Boroson, B. 2003, ApJ, 595, 719
Remillard, R. A., & McClintock, J. E. 2006, ARA&A, 44, 49
Reynolds, S. P. 2008, ARA&A, 46, 89
Soria, R., & Ghosh, K. K. 2009, ApJ, 696, 287
Tanaka, Y. 1997, in Proc. EARA Workshop, Accretion Disks—New Aspects, ed. E. Meyer-Hofmeister & H. Spruit (Lecture Notes in Physics, Vol. 487; Berlin: Springer), 1
Trudolyubov, S., Kotov, O., Priedhorsky, W., Cordova, F., & Mason, K. 2005, ApJ, 634, 314
van Speybroeck, L., Epstein, A., Forman, W., Giacconi, R., Jones, C., Liller, W., & Smarr, L. 1979, ApJ, 234, L45
Waller, W. H., et al. 2001, AJ, 121, 1395
White, N. E. 1989, A&AR, 1, 85